Miniemulsion Copolymerizations of Styrene and Methyl Methacrylate in the Presence of Reactive Costabilizer

C. S. Chern, H. Lim, N. A. Cala

Department of Chemical Engineering, National Taiwan University of Science and Technology, Taipei, 106 Taiwan

Received 17 June 2008; accepted 1 September 2008
DOI 10.1002/app.29279
Published online 22 December 2008 in Wiley InterScience (www.interscience.wiley.com).

ABSTRACT: Miniemulsion stability of three-component disperse phase systems comprising styrene [ST (1)], methyl methacrylate [MMA (2)], and stearyl methacrylate [SMA (3)] was investigated. The Ostwald ripening rate (ω) increases with increasing MMA content in the monomer mixture. The empirical equation $1/\omega = k(\varphi_1/\omega_1 + \varphi_2/\omega_2) + \varphi_3/\omega_3$ was proposed to adequately predict the miniemulsion stability data. The empirical parameter k was determined to be 555.77, and the Ostwald ripening rate (ω_3) and water solubility of SMA were estimated to be 8.77×10^{-21} cm^3/s and 1.90×10^{-9} mL/mL, respectively. A water-insoluble dye was used as a molecular probe to study particle nucleation mechanisms in the miniemulsion copolymerizations. In addition to the primary monomer droplet nucleation, homogeneous nucleation also plays an important role in the formation of particle nuclei, and this mechanism becomes more important for the polymerization systems with higher MMA contents as a result of the enhanced aqueous phase polymer reactions. The polymer composition data suggest that, during the early stage of polymerization, MMA is consumed more rapidly by free radical polymerization compared with ST. The final latex particle surface potential data also support this conclusion.
© 2008 Wiley Periodicals, Inc. J Appl Polym Sci 112: 173–180, 2009

Key words: miniemulsion polymerization; three-component disperse phase systems; Ostwald ripening; kinetics; particle nucleation

INTRODUCTION

Miniemulsions are thermodynamically unstable and they tend to undergo Ostwald ripening and/or coalescence processes to reduce the total oil-water interfacial area (i.e., total free energy). If adequately stabilized against coalescence, the former would be the predominant factor that is responsible for the substantial degradation of miniemulsion droplets. Ostwald ripening is the growth of large droplets with lower chemical potential at the expense of small droplets with higher chemical potential.[1,2] As a result of such a diffusional degradation process, the average droplet diameter increases upon aging.

Based on the Lifshitz-Slyozov-Wagner (LSW) theory, the Ostwald ripening rate can be expressed as[3,4]

$$\omega = d(d_m^3)/dt = 64D\sigma C_\infty V_m/(9RT) \quad (1)$$

where ω is the Ostwald ripening rate for single component species (cm^3/s), d_m the average oil droplet diameter (cm), C_∞ the water solubility of the bulk oil (mL/mL), V_m the molar volume of oil (cm^3/mol), D the diffusion coefficient of oil molecules in water, σ the interfacial tension at the oil-water interface (dyn/cm), T the absolute temperature (K), and R the gas constant. Equation (1) predicts that the Ostwald ripening rate is linearly proportional to the water solubility of the bulk monomer. Kabalnov et al.[5] experimentally confirmed this prediction for a series of *n*-alkanes stabilized by sodium lauryl sulfate (SLS).

Higuchi and Misra[6] were the first to show that oil-in-water (O/W) emulsions can be stabilized against Ostwald ripening by the incorporation of a highly water-insoluble compound (costabilizer) via the osmotic pressure effect. Since then, a number of studies were carried out to gain a better understanding of the qualitative and quantitative aspects of Ostwald ripening in the presence of costabilizer.[7–12] Kabalnov et al. developed an equation describing the Ostwald ripening rate for two-component disperse-phase miniemulsion systems based on the assumption of fast diffusion (ideal mixing) of the constituent components inside the droplets.[2]

$$1/\omega = (\varphi_1/\omega_1) + (\varphi_2/\omega_2) \quad (2)$$

where ω is the Ostwald ripening rate for the two-component disperse-phase system, ω_i ($i = 1$ or 2) the Ostwald ripening rate corresponding to the single component species i, and φ_i the volume fraction of the component i. When the water solubility of costabilizer is nil (i.e., ω_2 is extremely small), the first

Correspondence to: C. S. Chern (cschern@mail.ntust.edu.tw).

© 2008 Wiley Periodicals, Inc.

term in the denominator on the right hand side of eq. (2) can be neglected and, thus, it is the costabilizer that controls the Ostwald ripening process.

In conventional emulsion polymerization, free radical chain polymerization primarily takes place in discrete monomer-swollen polymer particles (i.e., reaction loci, about 10^1–10^2 nm in diameter) dispersed in a continuous aqueous phase. Although the particle nucleation period is quite short, it is the most important stage in emulsion polymerization. The total number of particle nuclei per unit volume of water, which has a significant influence on the polymerization kinetics, is mainly generated in this interval. The particle nucleation mechanisms generally accepted in the literature include micellar nucleation[13,14] and homogeneous nucleation.[15–18] According to micellar nucleation mechanism, it was proposed that latex particles (about 10^{-2}–10^1 μm in diameter, 10^{16}–10^{18} $1/dm^3$ in number density) form via the capture of free radicals generated in the continuous aqueous phase by monomer-swollen micelles, which exhibit an extremely large oil-water interfacial area. By contrast, for homogeneous nucleation, waterborne initiator radicals first form by the thermal decomposition of initiator and they can grow in size via the propagation reaction with those monomer molecules dissolved in the continuous aqueous phase. The oligomeric radicals then become water-insoluble when the critical chain length is reached. The hydrophobic oligomeric radical may thus coil up and form a particle nucleus in the continuous aqueous phase. This is followed by the formation of stable primary particles via the limited flocculation of the relatively unstable particle nuclei to reduce the total oil-water interfacial area and adsorption of surfactant molecules on their particle surfaces to increase the particle surface charge density.

In general, monomer droplets are not effective in competing with micelles in capturing free radicals due to the relatively small total droplet surface area. However, homogenized submicron monomer droplets containing an extremely hydrophobic, low-molecular-weight compound such as hexadecane, cetyl alcohol or a small amount of polymer may become the predominant particle nucleation loci (monomer droplet nucleation). This polymerization technique is termed as miniemulsion polymerization.[19–31] In our previous work,[9,30] alkyl methacrylates [e.g., stearyl methacrylate (SMA)] were used as reactive costabilizer to stabilize homogenized monomer droplets. The methacrylate group of costabilizer can be chemically incorporated into latex particles during the subsequent free radical polymerization. Furthermore, an extremely hydrophobic dye was incorporated into the droplets to investigate particle nucleation mechanisms in our previous work.[31–35] The authors first carried out a conventional emulsion polymerization to study the mass transfer of dye molecules, which were added to the reaction mixture at a monomer conversion of 32.4%, from the dye bulk phase to the growing latex particles. The experimental data show that transport of dye species from the bulk phase, across the continuous aqueous phase, and then into the reaction loci (i.e., latex particles) is insignificant due to the very low solubility of the dye in water. This result also eliminates the possibility of forming another population of monomer droplets incorporated with dye via the diffusion of dye molecules from latex particles into the continuous aqueous phase. This is because the extremely hydrophobic dye molecules are content with being buried inside the latex particles and, perhaps, the diffusion coefficient of dye with a molecular weight of 10^3 g/mol in a highly viscous polymeric matrix is not large enough to allow the desorption process to occur. A mass balance was then established to determine the number of latex particles (containing dye) per unit volume of water originating from monomer droplet nucleation and the number of primary particles (not containing dye) per unit volume of water generated in the continuous aqueous phase. However, the accuracy of this method relies on producing a stable monomer miniemulsion during polymerization. The experimental data thus obtained from this series of studies should be considered only as qualitative. Nevertheless, the amount of dye ultimately incorporated into the latex particles provides valuable information of the extent of monomer droplet nucleation. It was shown that the Ostwald ripening rate is the key factor that governs the probability of homogeneous nucleation occurring in a particular miniemulsion polymerization system. As a rule of thumb, the extent of homogeneous nucleation increases with increasing Ostwald ripening rate. This is because the Ostwald ripening process, which allows the transport of monomer molecules among droplets of different sizes, promotes the polymer reactions in the continuous aqueous phase.

The objective of this work was to study the effects of Ostwald ripening on the stability and subsequent polymerization of miniemulsions comprising ST (1) and MMA (2) with varying compositions in combination with a reactive costabilizer SMA (3). The surfactant concentration was kept constant below its critical micelle concentration (CMC) throughout this work. In this manner, micellar nucleation can be eliminated from the three-component disperse phase miniemulsion polymerization systems. It is of great interest to examine the general validity of the extended Kabalnov equation shown below.

$$1/\omega = (\varphi_1/\omega_1) + (\varphi_2/\omega_2) + (\varphi_3/\omega_3) \qquad (3)$$

The particle nucleation mechanisms involved in these three-component disperse phase miniemulsion polymerization systems are also the major focus of this work.

EXPERIMENTAL

Materials

The chemicals used include ST (Taiwan Styrene Co), MMA (Kaohsiung Monomer Co), SMA (Aldrich), sodium lauryl sulfate (SLS, J.T. Baker, 99%), sodium persulfate (SPS, Riedel de Haen), sodium bicarbonate (Riedel de Haen) as buffer, hydroquinone (HQ, Nacalai Tesque) as inhibitor and a dye (Blue 70, Shenq-Fong Fine Chemical, China). Other reagents used include methanol, ethanol, acetone, *n*-methyl pyrolidone (NMP), *d*-chloroform, pure nitrogen gas, magnesium sulfate anhydrous (Yakuri Chemicals), and deionized water (Barnsted, Nanopure Ultrapure Water System, specific conductance <0.057 μs/cm). ST and MMA were distilled under reduced pressure. Other chemicals were used as received.

Preparation of miniemulsion

The miniemulsion containing ST, MMA, and SMA was prepared by dissolving SLS in water and SMA in the monomer mixture, respectively. The oily and aqueous solutions were mixed using a mechanical agitator at 400 rpm for 10 min. The resultant emulsion was then homogenized with an ultrasonic homogenizer (Misonic sonicator 3000) for six cycles of 5 min in length with 2 min off-time, output power set at 60% (30 W). A typical miniemulsion formulation comprises (1) the continuous phase: 190 g of water, 2.66 m*M* of sodium bicarbonate and 5 m*M* of SLS; (2) the monomer charge: 50 g of monomers (ST and MMA), dye (0.1 wt % based on total monomer) and 20 m*M* of SMA; (3) the initiator solution: 10 g of water and sodium persulfate (0.3 wt % based on total monomer). The variable chosen for study is the weight ratio of ST to MMA (ST/MMA (w/w) = 100/0, 75/25, 50/50, 25/75, 0/100). For comparison, the two-component disperse phase miniemulsions (ST/MMA = 100/0 and 0/100) were also included in this study.

The average monomer droplet size data were determined by dynamic light scattering (DLS; LPA, Photal LPA-3000/3100). The sample was diluted with water to adjust the number of photons counted per second (cps) to 8000–12000. The dilution water was saturated with SLS and monomers and, consequently, diffusion of SLS and monomers from monomer droplets into the continuous aqueous phase was prohibited.

Miniemulsion polymerization

Immediately after homogenization, the resultant miniemulsion was charged into a 500-mL reactor equipped with a four-bladed fan turbine agitator, a thermocouple, and a reflux condenser and then purged with N_2 for 10 min while the temperature was brought to 70°C. The initiator solution was then charged into the reactor to start the polymerization. The reaction temperature was kept constant at 70°C and the agitation speed at 250 rpm. The latex product was filtered through 40-mesh (0.42 mm) and 200-mesh (0.074 mm) screens in series to collect filterable solids. Scraps adhering to the agitator, thermometer, and reactor wall were also collected.

The total solids content and conversion of monomers (X) were determined gravimetrically. The average particle diameter and polydispersity index (PDI) of the polymer particles were measured by TEM (JEOL, TEM-1200 EXII). The zeta potential (ζ) of latex particles was determined by Zetamaster (Malvern). The latex samples taken during polymerization were first coagulated by the addition of magnesium sulfate. Unincorporated dye, residue initiator and monomers, surfactant, inhibitor, and magnesium sulfate were washed away using methanol by mixing in a supersonic cleaner. Precipitated polymer particles were then rinsed twice with an excess of water. Approximately 0.1 g of dried polymer was dissolved in 20 mL of NMP for the determination of the dye content by the ultraviolet (UV) absorbance method (Shimadzu, UV-160A). The extinction coefficient obtained from the calibration curve of the characteristic UV absorbance at 675 nm versus the dye concentration (0–1.4×10^{-5} g/mL) data was 8.6633 $\times 10^4$ mL/(cm g). The reported weight percentage of dye ultimately incorporated into latex particles (P_{dye}) represents the average of six measurements. The copolymer composition data obtained from ^{1}H-NMR (Varian Gemin 2000, 500 MHz) were used to calculate the individual monomer conversions.

RESULTS AND DISCUSSION

Miniemulsion stability

The extended LSW theory[8] was used to determine the Ostwald ripening rate (ω) for the three-component disperse phase miniemulsion systems upon aging at 30°C; the slope obtained from the least-squares best fitted d_m^3-versus-time straight line was taken as ω, as shown in Figure 1. The relatively low values of the coefficient of determination (R^2) reflect the rather scattered miniemulsion stability data based on the dynamic light scattering technique. How to accurately measure the liquid droplet size represents a great challenge to colloidal scientists. The experimental data of ω as a function of the

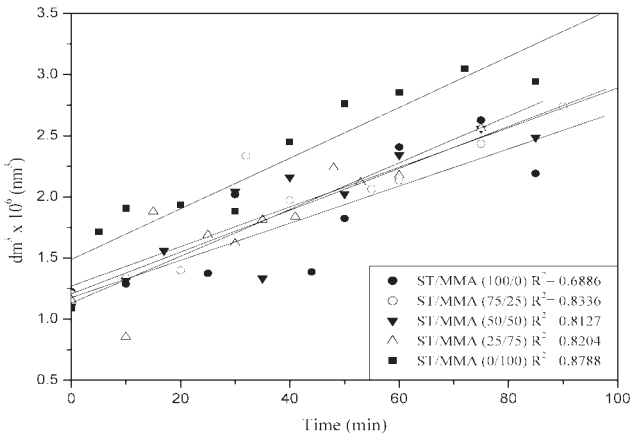

Figure 1 Average monomer droplet diameter as a function of time for miniemulsion samples with varying monomer compositions stabilized by SLS and SMA upon aging at 30°C. ST/MMA (w/w) = (●) 100/0; (○) 75/25; (▼) 50/50; (△) 25/75; (■) 0/100.

weight fraction of MMA in the monomer mixture is shown by the discrete circular data points in Figure 2. As expected, the Ostwald ripening rate increases with increasing MMA content (water solubility in decreasing order: MMA > ST ≫ SMA).

The extended Kabalnov model [eq. (3)] was first used to predict the Ostwald ripening behavior for the three-component disperse phase systems. The Ostwald ripening rate data for the constituent components ST ($\omega_{ST} = 4.99 \times 10^{-16}$ cm^3/s) and MMA ($\omega_{MMA} = 3.97 \times 10^{-14}$ cm^3/s) were obtained from Ref. [12]. Based on eq. (2), the average Ostwald ripening rate of SMA (ω_{SMA}) was estimated to be (7.98 ± 1.31) $\times 10^{-21}$ cm^3/s by the Ostwald ripening rate data of the two runs (ST/MMA = 100/0 and 0/100) along with the above-mentioned ω_{ST} and ω_{MMA} values. The extended Kabalnov equation fails to predict the Ostwald ripening behavior, as shown by the dotted line in Figure 2. The next approach was to treat the three-component disperse phase system simply as a pseudotwo-component system; the mixture of ST and MMA was regarded as component 1, and SMA component 2 in eq. (2). The water solubility of the mixture of ST and MMA (C_{mix}) was estimated by the relationship $C_{mix} = x_{ST}C_{ST} + x_{MMA}C_{MMA}$, where x_{ST} and x_{MMA} are the mole fractions of ST and MMA, respectively, and $C_{ST} = 1.94 \times 10^{-4}$ mL/mL and $C_{MMA} = 1.60 \times 10^{-2}$ mL/mL are the water solubilities of the two bulk monomers, respectively.[12] The C_{mix} value was used to estimate the Ostwald ripening rate ($\omega_{ST/MMA}$) according to the correlation established.[12] With the knowledge of $\omega_{ST/MMA}$ and ω_{SMA}, the Ostwald ripening rate of the pseudotwo-component system was then calculated based on eq. (2). Again, the model predictions deviate significantly from the experimental data (see the dashed line in Fig. 2). Both the extended Kabalnov and pseudotwo-component models show that the Ostwald ripening rate is insensitive to changes in the monomer composition owing to the predominant retardation of Ostwald ripening by SMA. The mechanism responsible for the failure of these two models in predicting the colloidal stability of the miniemulsion systems investigated in this work is not clear at this point of time.

The following empirical equation was then proposed in an attempt to describe the Ostwald ripening behavior of the three-component disperse phase miniemulsion systems.

$$1/\omega = k(\varphi_1/\omega_1 + \varphi_2/\omega_2) + \varphi_3/\omega_3 \quad (4)$$

With k and ω_3 as the adjustable parameters, a plot of $1/\omega$ versus $[(\varphi_1/\omega_1) + (\varphi_2/\omega_2)]$ will result in a straight line with a slope of k and an intercept φ_3/ω_3. The least-squares best-fit technique led to values of k and ω_3 to be 555.77 and 8.77×10^{-21} cm^3/s, respectively, ($R^2 = 0.9805$, see the solid line in Fig. 2). This model describes the Ostwald ripening behavior for the three-component systems reasonably well. Based on the correlation reported in Ref. 12 and the best-fitted value of ω_3, the water solubility of SMA was estimated to be 1.90×10^{-9} mL/mL, which is comparable to the reported value (3.23×10^{-9} mL/mL).[10]

During the early stage of aging, the more hydrophilic MMA molecules are expected to diffuse first from smaller droplets into the continuous aqueous phase and then redeposit into larger ones. The more hydrophobic ST species may also participate early in the Ostwald ripening process, but in an insignificant fashion. Subsequently, the contribution of ST to

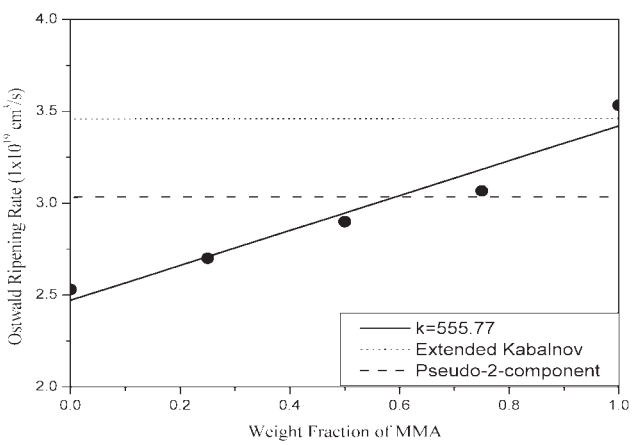

Figure 2 Ostwald ripening rate as a function of MMA weight fraction for miniemulsion samples with varying monomer compositions stabilized by SLS and SMA upon aging at 30°C. The discrete circular points represent the experimental data and the continuous curves represent the model predictions. (·····) extended Kabanov model; (- - -) pseudotwo-component model; (——) an empirical equation proposed in this work.

TABLE I
Some Kinetic Parameters Obtained from Miniemulsion Copolymerizations of ST and MMA in the Presence of SMA at 70°C

ST/MMA (*w*/*w*)	100/0	75/25	50/50	25/75	0/100
$R_p \times 10^2$ [mol/(L s)]	4.56	6.29	6.71	15.69	27.34
$d_{m,i}$ (nm)[a]	107.0	107.4	105.6	104.8	104.9
$d_{w,f}$ (nm)[b]	94.1	77.2	72.5	68.9	66.2
$d_{w,f}/d_{n,f}$[c]	1.04	1.09	1.05	1.11	1.19
$N_{m,i} \times 10^{17}$ (1/L)[d]	3.69	3.85	4.05	4.15	4.13
$N_{p,f} \times 10^{17}$ (1/L)[e]	4.77	7.27	11.40	12.49	14.13
$N_{p,f}/N_{m,i}$	1.29	1.89	2.81	3.01	3.42
$P_{dye,f}$ (%)[f]	89.4	76.2	71.8	59.5	55.0
Total scraps (%)	0.02	0.02	0.03	0.01	0.02

The subscript "i" represents initial, and "f" represents final.
[a] Initial monomer droplet diameter (DLS).
[b] Final weight-average latex particle diameter (TEM).
[c] Polydispersity index of final latex particle size distribution (TEM).
[d] Initial number of monomer droplets (DLS).
[e] Final number of latex particles (TEM).
[f] Final dye content.

Ostwald ripening becomes more important. The molecular degradation of droplets is alleviated when the osmotic pressure effect becomes strong enough to compete with the molecular degradation effect toward the end of the Ostwald ripening process. As to the extremely hydrophobic SMA, its contribution to Ostwald ripening can be neglected throughout the molecular degradation process.

Miniemulsion polymerization

In this series of copolymerizations of ST and MMA, the miniemulsion systems were stabilized by 5 m*M* of SLS and 20 m*M* of SMA (based on the aqueous phase). Polymerizations were initiated by a water-soluble initiator SPS at 70°C and the initiator concentration was kept constant (0.3 wt % based on total monomer weight) in this work. The average total scraps collected at the end of polymerization are about 0.02%, indicating satisfactory colloidal stability during polymerization (Table I). Figure 3 shows the overall monomer conversion (X) versus time profiles. In the presence of 20 m*M* of SMA, the polymerization rate for the run with ST/MMA = 0/100 is much faster than the counterpart with ST/MMA = 100/0. Furthermore, the polymerization rate increases with increasing MMA content in the monomer mixture. The water solubility of MMA (159 m*M*) is much higher than that of ST (1.92 m*M*). Therefore, the concentration of MMA in the continuous aqueous phase is higher in comparison with the ST counterpart. It is postulated that more particle nuclei (i.e., reaction loci) can be generated via both monomer droplet nucleation and homogeneous nucleation for the reaction system containing more MMA, thereby leading to a faster polymerization rate (polymerization rate is linearly proportional to the propagation rate constant and the number of latex particles per unit volume of water). Furthermore, the propagation rate constant of MMA is larger than that of ST.[36] Both factors support the observed trend.

Figure 4 shows the average colloidal particle diameter of the reaction mixture including the latex particles and monomer droplets versus overall monomer conversion profiles. Small differences in the initial monomer droplet size were observed for the miniemulsions with varying monomer compositions. It seems that the net power input during homogenization controls the initial monomer droplet size. Initially, the colloidal particle size decreases rapidly and then levels off with the progress of polymerization (Fig. 4). It should be noted that the polymerization was carried out at a SLS concentration

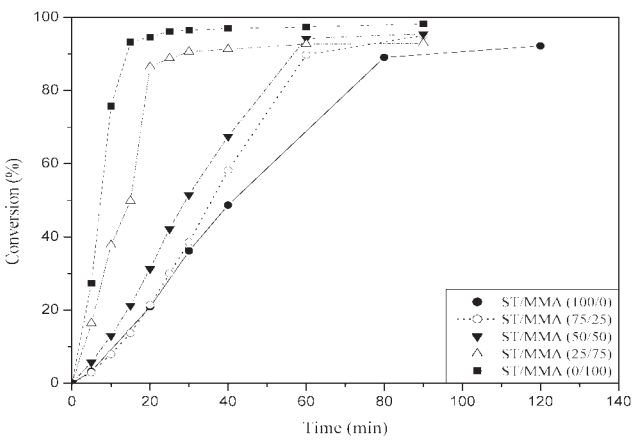

Figure 3 Monomer conversion as a function of time for miniemulsion polymerization samples with varying monomer compositions stabilized by SLS and SMA at 70°C. ST/MMA (*w*/*w*) = (●) 100/0; (○) 75/25; (▼) 50/50; (△) 25/75; (■) 0/100.

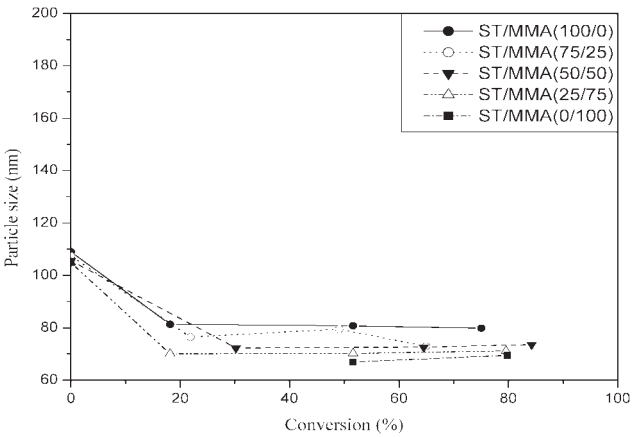

Figure 4 Average diameter of colloidal particles as a function of conversion for miniemulsion polymerization samples with varying monomer compositions stabilized by SLS and SMA at 70°C. ST/MMA (w/w) = (●) 100/0; (○) 75/25; (▼) 50/50; (△) 25/75; (■) 0/100.

(5 mM) below its CMC (8.2 mM[37]) to prevent the formation of micelles. During the early stage of polymerization (0% < X < 30%), the rapid decrease of particle size is most likely caused by the generation of particle nuclei with a diameter of less than 10 nm in the continuous aqueous phase via homogeneous nucleation. Generation of a second crop of tiny particle nuclei tends to reduce the average particle size of the colloidal system, which only contains monomer droplets with a diameter of about 100 nm at the very beginning of polymerization. After 30% conversion, the probability for latex particles with a very large total surface area to capture water-borne free radicals and particle embryos increases significantly and homogeneous nucleation is depressed accordingly. In addition, those latex particles originating from homogeneous nucleation continue to grow toward the end of polymerization. All these factors contribute to the relatively constant latex particle size observed during the latter stage of polymerization.

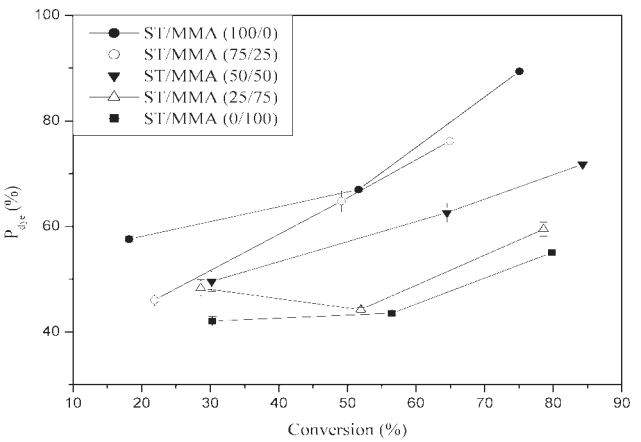

Figure 5 Percentage of dye ultimately incorporated into latex particles as a function of conversion for miniemulsion polymerization samples with varying monomer compositions stabilized by SLS and SMA at 70°C. ST/MMA (w/w) = (●) 100/0; (○) 75/25; (▼) 50/50; (△) 25/75; (■) 0/100.

The initial decrease of the average colloidal particle diameter is more pronounced in the polymerization system with a higher MMA content. Neglecting coalescence of monomer droplets, a value of $N_{p,f}/N_{m,i}$ equal to unity would imply that monomer droplets initially present in the polymerization system are all successfully nucleated during polymerization. The parameters $N_{m,i}$ and $N_{p,f}$ represent the total number of monomer droplets initially present in the reaction system and the total number of latex particles per unit volume of water at the end of polymerization, respectively. By contrast, a value of $N_{p,f}/N_{m,i}$ greater than unity would suggest that there must be other nucleation mechanisms (e.g., homogeneous nucleation) taking place beside monomer droplet nucleation. The experimental results show that all the values of $N_{p,f}/N_{m,i}$ are greater than one, even for the polymerization system with ST/MMA = 100/0, and the value of $N_{p,f}/N_{m,i}$ increases with increasing MMA content (Table I). It is then postulated that competitive particle nucleation mechanisms (monomer droplet nucleation and homogeneous nucleation) are operative in these three-component disperse phase systems. Furthermore, the degree of homogeneous nucleation increases with increasing MMA content in the monomer mixture.

A significant difference in the P_{dye} data was observed for the two polymerizations with ST/MMA = 100/0 and 0/100. Moreover, at constant overall monomer conversion, P_{dye} decreases with increasing MMA content in the monomer mixture (Table I and Fig. 5). The reproducibility of these P_{dye} data is quite satisfactory as shown by the error bars

TABLE II
Individual Monomer Conversion of ST and MMA for Miniemulsion Copolymerizations with Varying Compositions at 70°C

ST/MMA (w/w)	Overall conversion (%)	X_{ST} (%)[a]	X_{MMA} (%)[b]
	21.9	17.5	37.9
75/25	49.1	42.6	73.8
	65.0	60.6	83.8
	30.2	27.8	34.5
50/50	52.5	50.5	57.1
	75.1	71.0	82.0
	28.6	27.9	30.0
25/75	52.0	56.1	52.3
	78.6	71.3	82.9

[a] Individual conversion of ST.
[b] Individual conversion of MMA.

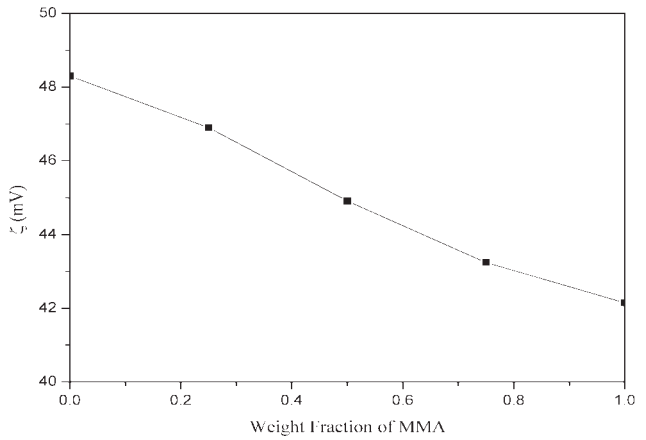

Figure 6 Zeta potential of final latex particles as a function of weight fraction of MMA for miniemulsion polymerization samples with varying monomer compositions stabilized by SLS and SMA at 70°C.

in Figure 5. P_{dye} increases with increasing conversion for all the polymerizations investigated in this work. This indicates that particle nuclei form continuously during the polymerization. Table I shows that $N_{m,i}$ increases with increasing MMA content. This will result in a higher probability for oligomeric radicals to enter monomer droplets and, thus, $P_{dye,f}$ is expected to increase for the polymerization system with a higher MMA content. However, this is not the case. The only possible explanation for the experimental results is the greatly enhanced formation of particle nuclei in the continuous aqueous phase when the MMA content is increased.

The polymer composition data at low (20–30%), medium ($\sim$ 50%) and high (65–80%) overall monomer conversion obtained from ^{1}H-NMR measurements and the calculated individual monomer conversion data are summarized in Table II. The consumption of MMA by free radical polymerization is always faster than ST, which is consistent with the kinetic data shown in Figure 3. Figure 6 shows the zeta potential (ζ) of the final latex particles data as a function of the MMA content in the monomer mixture. The ζ value decreases significantly as the MMA content is increased. This is because a larger population of smaller latex particles can be achieved in the polymerization system with a lower ST/MMA ratio (see the $N_{p,f}$ and $d_{w,f}$ data in Table I). At constant weight of monomers, the total particle surface area is inversely proportional to the particle size. Thus, at constant surfactant weight, the surface surfactant concentration (i.e., surface charge density or ζ) decreases with increasing MMA content. Another factor that comes into play is the increased particle surface polarity with MMA content. The higher the particle surface polarity, the smaller the amount of SLS that can be adsorbed on the latex particles. This will then result in a decreased surface charge density (or ζ) with MMA content.

CONCLUSIONS

The stability and subsequent free radical polymerization of the three-component disperse phase miniemulsions of varying monomer compositions (ST/MMA (w/w) = 100/0, 75/25, 50/50, 25/75, 0/100) in the presence of a reactive costabilizer SMA were investigated. For miniemulsion samples upon aging at 30°C, the Ostwald ripening rate increases with increasing MMA content in the monomer mixture. Both the extended Kabanov equation and pseudotwo-component equation failed to predict the Ostwald ripening rate data. The empirical model $1/\omega = k(\varphi_1/\omega_1 + \varphi_2/\omega_2) + \varphi_3/\omega_3$ can adequately predict the Ostwald ripening rate data over a wide range of monomer compositions. The empirical parameter k, ω_3, and the water solubility of SMA were estimated to be 555.77, 8.77×10^{-21} cm^3/s, and 1.9×10^{-9} mL/mL, respectively. A mechanism was proposed to describe the Ostwald ripening process involved in the three-component disperse phase miniemulsion system.

The kinetic studies showed that the polymerization rate increases rapidly with increasing MMA content in the monomer mixture. This is closely related to the nature of the constituent monomers (ST and MMA) and the particle nucleation mechanisms. The costabilizer SMA has a water solubility in the order of 10^{-9} mL/mL, but it is still not hydrophobic enough to completely eliminate the Ostwald ripening effect, thereby increasing the probability of polymer reactions occurring in the continuous aqueous phase. In addition to monomer droplet nucleation, particle nuclei can form in the continuous aqueous phase via homogeneous nucleation, even for the relatively hydrophobic monomer ST. The extent of homogeneous nucleation increases when the MMA content is increased.

References

1. Taylor, P. Colloids Surf A 1995, 99, 175.
2. Taylor, P. Adv Colloid Interface Sci 1998, 75, 107.
3. Lifshitz, I. M.; Slezov, V. V. J Phys Chem Solids 1961, 19, 35.
4. Wagner, C. Ber Bunsenges Phys Chem 1961, 65, 581.
5. Kabalnov, A. S.; Makarov, K. N.; Pertzov, A. V.; Shchukin, E. D. J Colloid Interface Sci 1990, 138, 98.
6. Higuchi, W. I.; Misra, J. J Pharm Sci 1962, 51, 459.
7. Choi, Y. T. Formation and Stabilization of Miniemulsion and Latexes, PhD Dissertation, Lehigh University, Betlehem, 1986.
8. Kabalnov, A. S.; Pertzov, A. V.; Shchukin, E. D. Colloids Surf 1987, 24, 19.
9. Chern, C. S.; Chen, T. J Colloid Polym Sci 1997, 275, 546.
10. Chern, C. S.; Chen, T. J Colloid Surf A 1998, 138, 65.
11. Blythe, P. J.; Morrison, B. R.; Mathauer, K. A.; Sudol, E. D.; El-Aasser, M. S. Langmuir 2000, 16, 898.

12. Tauer, K. Polymer 2005, 46, 1385.
13. Harkins, W. D. J Am Chem Soc 1947, 69, 1428.
14. Smith, W. V.; Ewart, R. W. J Chem Phys 1948, 16, 529.
15. Jacobi, B. Angew Chem 1952, 64, 539.
16. Priest, W. J. J Phys Chem 1952, 56, 1077.
17. Fitch, R. M.; Tsai, C. H. Polymer Colloids; Fitch, R. M., Ed.; Plenum: New York, 1980; p 73.
18. Roe, C. P. Ind Eng Chem 1968, 60, 20.
19. Ugelstad, J.; El-Aasser, M. S.; Vanderhoff, J. W. J Polym Sci 1973, 11, 503.
20. Ugelstad, J.; Hansen, F. K.; Lange, S. Makromol Chem 1974, 175, 507.
21. Hansen, F. K.; Ugelstad, J. J Polym Sci Polym Chem 1979, 17, 3069.
22. Chamberlain, B. J.; Napper, D. H.; Gilbert, R. G. J Chem Soc Faraday Trans 1982, 78, 591.
23. Choi, Y. T.; El-Aasser, M. S.; Sudol, E. D.; Vanderhoff, J. W. J Polym Sci Polym Chem 1985, 23, 2973.
24. Delgado, J.; El-Aasser, M. S.; Vanderhof, J. W. J Polym Sci Part A: Polym Chem 1986, 24, 861.
25. Wang, S.; Schork, F. J. J Appl Polym Sci 1994, 54, 2157.
26. Saethre, B.; Mork, P. C.; Ugelstad, J. J Polym Sci Part A: Polym Chem 1995, 33, 2951.
27. Reimers, J.; Schork, F. J. J Appl Polym Sci 1996, 59, 1833.
28. Reimers, J.; Schork, F. J. J Appl Polym Sci 1996, 60, 251.
29. Huang, H.; Zhang, H.; Li, J.; Cheng, S.; Hu, F.; Tan, B. J Appl Polym Sci 1998, 68, 2029.
30. Chern, C. S.; Chen, T. J Colloid Polym Sci 1997, 275, 1060.
31. Chern, C. S.; Chen, T. J.; Liou, Y. C. Polymer 1998, 39, 3767.
32. Chern, C. S.; Liou, Y. C. Macromol Chem Phys 1998, 199, 2051.
33. Chern, C. S.; Liou, Y. C. Polymer 1999, 40, 3763.
34. Chern, C. S.; Liou, Y. C. J Polym Sci Polym Chem Ed 1999, 37, 2537.
35. Chern, C. S.; Principles and Applications of Emulsion Polymerization; Wiley: New York, 2008; pp 137, 138.
36. Brandrup, J.; Immergut, E. H., Eds. Polymer Handbook, 3rd ed.; Wiley: New York, 1989; II/71–73, 75, 76.
37. Rehfeld, S. J. J Phys Chem 1967, 71, 738.